JOURNAL OF AEROSPACE INFORMATION SYSTEMS
Vol. 17, No. 8, August 2020

Multiple-Pursuer, Single-Evader Border Defense Differential Game

Alexander Von Moll,* Eloy Garcia,* and David Casbeer*
Air Force Research Laboratory, Wright–Patterson Air Force Base, Ohio 45433
and
M. Suresh† and Sufal Chandra Swar†
Aeronautical Development Establishment, Bangalore 560 075, India

https://doi.org/10.2514/1.I010740

Ensuring border security against potential threats has been a long-standing problem, and it becomes much more challenging for international borders due to their massive physical extent coupled with varied terrain. This paper considers a scenario in which a team of UAVs (the pursuers) attempt to prevent an intruder ground vehicle (the evader) from escaping through the border. The ground intruder's presence is made known by a laser fence positioned inside the border. Upon detection, the UAVs are activated and given the objective to cooperatively capture the intruder. This paper formulates the scenario as a zero-sum differential game whereupon all agents exhibit simple motion and the pursuers have a speed advantage. For cases where capture inside the border is possible, the payoff/cost for the pursuers/evader is the distance from capture to the border. The solution to the game is derived based on the geometric properties of the game and verified for the single-pursuer case with a border comprising straight-line segments. This game may contain a dispersal surface that has interesting practical consequences when the optimal strategies are applied in discrete time.

Nomenclature

B	=	border
C	=	Apollonius circle center
$\mathcal{C}$	=	set of termination conditions
D	=	Apollonius disk
F	=	point on the border that is closest to the capture point
I	=	candidate capture point
I^*	=	optimal capture point
J	=	cost (payoff) for evader (pursuers)
$\mathcal{R}_E$	=	region of win for the evader
$\mathcal{R}_P$	=	region of win for the pursuer(s)
r	=	Apollonius circle radius
S	=	Evader's feasible region
V	=	value of the game
V_E	=	evader speed
V_P	=	pursuer speed
$\boldsymbol{x}$	=	system state
α	=	ratio of evader speed to pursuer speed
ϕ	=	evader's heading angle
ψ_i	=	pursuer i's heading angle

I. Introduction

BORDER surveillance and defense is a task for which UAVs are well-suited to carry out as it requires persistent vigilance. Additionally, their relative speed compared with ground vehicles and the possibility of varied terrain points to the utility of UAVs for this purpose. One possible scenario pertaining to border surveillance and defense is that of an intruder, perhaps performing surveillance for the enemy, which, having gathered some information, is now attempting to escape back to safety through the border to deliver the acquired information. Thus we are interested in engaging the intruder with a number of homogeneous UAVs with the intent of capturing the intruder or at least destroying it within the border. Conceptually, the border may represent a physical border and thus capture of a vehicle outside the border could be considered an act of war, or perhaps the border represents our sensor range, outside of which the intruder's position cannot be tracked. Suppose that the intruder is a ground vehicle, or UAV, whose maximum speed is less than the speed of our UAVs—thus capture may be possible in some situations. If the intruder's speed is greater, then capture may not ever be possible. The presence of the intruder is made known to the UAVs by an event such as the intruder crossing a laser fence. From this point on, the position of the intruder is known to the UAVs. The goal, then, is for the UAVs to cooperate in capturing the intruder based on their positions at the time the laser fence is crossed by the intruder. Here, capture is achieved when one or more UAVs are coincident with the intruder.

We formulate the above scenario as a differential game wherein the agents have simple motion; that is, the vehicles are not turn-constrained and have a fixed speed. This problem may be categorized as pursuit-evasion, where our UAVs play the role of the pursuers and the intruder serves as the evader. Pursuit-evasion differential games were explored extensively by Isaacs in [1]. Recently, there has been much work in analyzing these types of problems—for instance, [2] re-examined Isaacs's two cutters and fugitive ship problem, in which two fast pursuers cooperate to capture a single evader, and the cost is capture time. The solution was then generalized in [3] for any number of pursuers. Other contributions have focused on introducing additional complexity by including a constrained environment [4,5] or adding obstacles [6,7]. In all of the cases mentioned above, capture time is the payoff/cost of the game. Thus the evader is interested only in extending its life. The so-called games of approach, wherein the evader is faster than the pursuers, use a different payoff/cost, but the saddle point strategies end up being similar (i.e., aiming at a static point) [8]. In the present scenario, the evader seeks to escape, if possible, or to minimize its distance to the border at capture if it cannot escape. This scenario is similar to one considered by Isaacs, which he referred to as *Guarding a target* (see Example 1.9.2 in [1]). The analogy is that the border serves as the target; the difference is the presence of multiple pursuers (or guards) and their speed advantage over the evader.

Two questions (or games) may be considered in this scenario: 1) Is escape possible for the evader (the game of kind)? 2) How close can the evader get to the border before being captured (the game of degree)? In the remainder of this paper, both games will be addressed. Section II expresses the problem formulation of the game of degree. Section III describes the game of kind and characterizes the win regions for the single- and multiple-pursuer cases. Section IV

Presented as Paper 2019-1162 at the 2019 AIAA SciTech Forum, San Diego, CA, January 7–11, 2019; received 29 March 2019; revision received 26 December 2019; accepted for publication 3 January 2020; published online 5 February 2020.

*Research Engineer, Controls Science Center of Excellence, 2210 8th St.
†Scientist, Autonomous Cooperative Systems Laboratory, New Thippasandra Post.

discusses the possibility for a dispersal surface in the game and some practical consequences. Lastly, Sec. V concludes this work and discusses some possible extensions.

II. Game of Degree

Here we consider the game of degree wherein escape through the border is not possible for evader. Consider M pursuers and an evader, with simple motion in the $\mathbb{R}^2$ plane:

$$\begin{aligned} \dot{x}_E &= \alpha \cos\phi, \\ \dot{y}_E &= \alpha \sin\phi, \\ \dot{x}_{P_i} &= \cos\psi_i, \qquad i = 1,\ldots,M \\ \dot{y}_{P_i} &= \sin\psi_i, \qquad i = 1,\ldots,M \end{aligned} \tag{1}$$

where $\alpha = V_E/V_P < 1$ is the speed ratio constant; note that the pursuers share the same velocity $V_{P_i} = V_P$, $i = 1,\ldots,M$. The admissible controls are given by $\phi, \psi_i \in [-\pi, \pi]$. The cost/payoff function is the terminal distance, at the time of interception, between the evader and the border. The pursuer strives to capture the evader and maximize this separation, whereas the evader wants to minimize it. The cost/payoff function can be written as follows:

$$J = \sqrt{(x_{E_f} - x_F)^2 + (y_{E_f} - y_F)^2} \tag{2}$$

where the point F: (x_F, y_F) is defined as the point on (any segment of) the border that is the closest to the terminal position of the evader.

Interception is defined by point capture; that is, the game terminates when the state of the system enters the set

$$\mathcal{C} := \left\{ \boldsymbol{x} \middle| \exists i \text{ s.t. } \sqrt{(x_{P_i} - x_E)^2 + (y_{P_i} - y_E)^2} = 0 \right\} \tag{3}$$

Figure 1 specifies the coordinate system as well as the payoff/cost for a given interception point (x_{E_f}, y_{E_f}). The main point of defining the objective in Eq. (2) this way is robustness to uncertainty, in terms of both the opponents' strategy as well as the environment. The pursuers want to keep the evader as far from the border as possible in case a pursuer is incapacitated or blown off-course by wind, which could allow the evader to get closer to the border or even escape. For some applications, whether or not escape occurs is the only thing that matters. However, by solving the Game of Degree, the pursuers give themselves the best shot at capturing the evader in the face of uncertainty in the environment and in the evader's implemented control.

A. Single-Pursuer Solution and Verification

In this differential game we can then define an Apollonius circle using the instantaneous separation between P (pursuer) and E (evader) and the speed ratio parameter $\alpha = V_E/V_P < 1$. Let C denote the center of the circle. We have that three points, P, E, and C, are located on the same line; see Fig. 2. Also in this figure we can see that the borderline separates the plane into two regions. The game is played in the region of the Euclidean plane $\mathcal{G}$, where both the pursuer and the evader are initially located. This region is further divided into the region of win for the pursuers and the region of win of the evader.

Define $d = \sqrt{(x_E - x_P)^2 + (y_E - y_P)^2}$ as the distance between players P and E. Also, let r be the radius of the Apollonius circle. Then, r is given by

$$r = \frac{\alpha}{1 - \alpha^2} d \tag{4}$$

Assume that the parameters (m_i, n_i) of each border segment are given, where the segment i is given by $y = m_i x + n_i$. Also assume that the $\boldsymbol{x} \in \mathcal{R}_P$, that is, in the region of win of the pursuer. $\mathcal{R}_P$ can be determined by analyzing whether or not the Apollonius circle intersects any segment of the border.

Proposition 1: Consider the differential game of border defense [Eqs. (1–3)]. The Value function is given by $V(\boldsymbol{x}) = V_{i^*}(\boldsymbol{x})$, where $i^* = \arg\ \min_i V_i(\boldsymbol{x})$ and

$$\begin{aligned} V_i(\boldsymbol{x}) = \frac{1}{1-\alpha^2}\Bigg[&\left(x_E - \alpha^2 x_P - m_i \frac{y_E - \bar{m}_i x_E - \alpha^2(y_P - \bar{m}_i x_P) - (1-\alpha^2) n_i}{m_i^2 + 1} \right)^2 \\ &+ \left(y_E - \alpha^2 y_P - m_i^2 \frac{y_E - \bar{m}_i x_E - \alpha^2(y_P - \bar{m}_i x_P) + [(1-\alpha^2)/m_i^2] n_i}{m_i^2 + 1} \right)^2 \Bigg]^{1/2} \\ &- \frac{\alpha}{1-\alpha^2} [(x_E - x_P)^2 + (y_E - y_P)^2]^{1/2} \end{aligned} \tag{5}$$

where $\boldsymbol{x} = [x_E \quad y_E \quad x_P \quad y_P]^T$.

Proof: The optimal cost/payoff is obtained when E is intercepted by P at the point on the Apollonius circle closest to the border. For

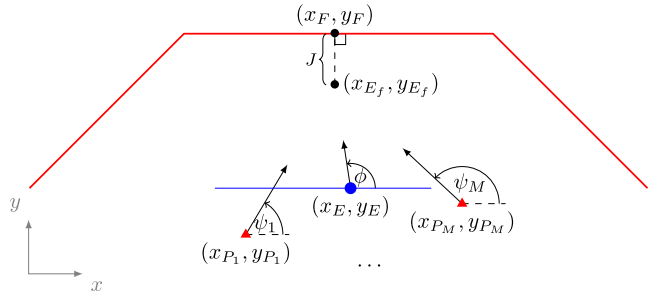

Fig. 1 Definition of scenario, coordinate system, and payoff/cost. Red triangles represent pursuers, the blue circle is the evader, the blue line is the laser fence, and the red line is the border.

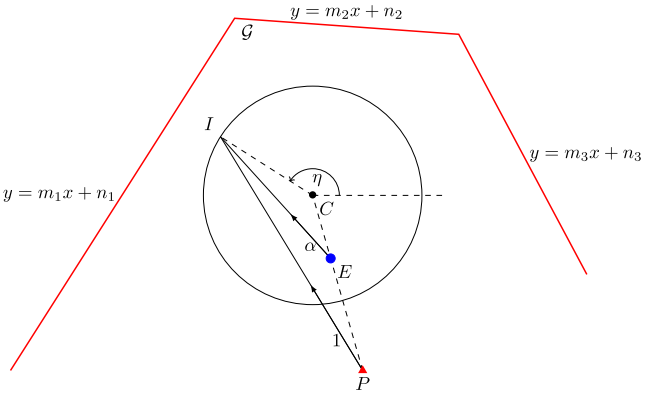

Fig. 2 Border defense scenario 1 pursuer–1 evader.

each segment of the border, the closest point between the circle and the border segment is given by the orthogonal line to the border segment that passes by the center of the circle C as shown in Fig. 3. The distance between points I_i and F_i is given by

$$V_i(\boldsymbol{x}) = \sqrt{(x_c - x_F)^2 + (y_c - y_F)^2} - r \tag{6}$$

where the center of the circle is explicitly given by

$$\begin{aligned} x_c &= \frac{1}{1-\alpha^2}(x_E - \alpha^2 x_P) \\ y_c &= \frac{1}{1-\alpha^2}(y_E - \alpha^2 y_P) \end{aligned} \tag{7}$$

To write the Value function directly in terms of the state $\boldsymbol{x}$ we need to evaluate the point F: (x_F, y_F) in terms of the state $\boldsymbol{x}$. The equation of the orthogonal line to segment i passing through C is $y = \bar{m}_i x + \bar{n}_i$, where $\bar{m}_i = -(1/m_i)$ and

$$\begin{aligned} \bar{n}_i(\boldsymbol{x}) &= y_c - \bar{m}_i x_c \\ &= \frac{1}{1-\alpha^2}(y_E - \alpha^2 y_P - \bar{m}_i(x_E - \alpha^2 x_P)) \end{aligned} \tag{8}$$

We now solve the following linear equation to determine x_F

$$m_i x_F + n_i = \bar{m}_i x_F + \bar{n}_i$$

The coordinate x_F is explicitly given by

$$\begin{aligned} x_F(\boldsymbol{x}) &= \frac{\bar{n}_i - n_i}{m_i - \bar{m}_i} \\ &= \frac{m_i}{1-\alpha^2} \cdot \frac{y_E - \bar{m}_i x_E - \alpha^2(y_P - \bar{m}_i x_P) - (1-\alpha^2)n_i}{m_i^2 + 1} \end{aligned} \tag{9}$$

and y_F is given by

$$\begin{aligned} y_F(\boldsymbol{x}) &= m_i x_F + n_i \\ &= \frac{m_i^2}{1-\alpha^2} \cdot \frac{y_E - \bar{m}_i x_E - \alpha^2(y_P - \bar{m}_i x_P) + [(1-\alpha^2)/m_i^2]n_i}{m_i^2 + 1} \end{aligned} \tag{10}$$

Substitute Eqs. (4), (7), (9), and (10) into Eq. (6) to obtain Eq. (5). The problem of finding the closest point on the border to the Apollonius circle has been simplified by obtaining the closest point of each segment of the border to the Apollonius circle. Then, the solution is given by $i^* = \arg\ \min_i V_i(\boldsymbol{x})$. □

In the next theorem we have removed the subscript i for simplicity; that is, it is assumed that the optimal segment i has been determined.

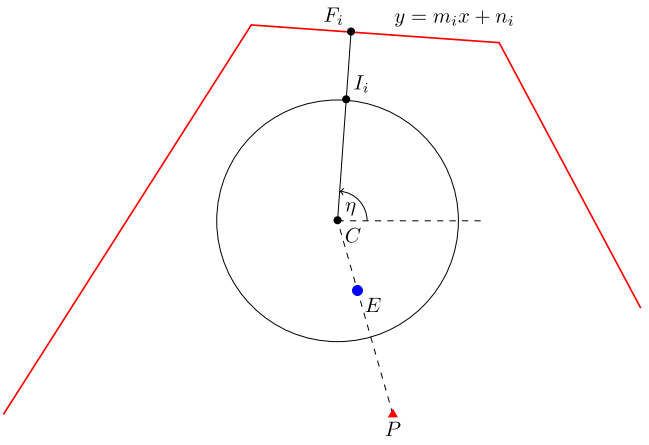

Fig. 3 Derivation of $V(\boldsymbol{x})$.

Theorem 1: Consider the differential game of border defense [Eqs. (1–3)]. The saddle point strategies of the evader and the pursuer are

$$\begin{aligned} \cos\phi^* &= \frac{x_I - x_E}{\sqrt{(x_I - x_E)^2 + (y_I - y_E)^2}} \\ \sin\phi^* &= \frac{y_I - y_E}{\sqrt{(x_I - x_E)^2 + (y_I - y_E)^2}} \\ \cos\psi^* &= \frac{x_I - x_P}{\sqrt{(x_I - x_P)^2 + (y_I - y_P)^2}} \\ \sin\psi^* &= \frac{y_I - y_P}{\sqrt{(x_I - x_P)^2 + (y_I - y_P)^2}} \end{aligned} \tag{11}$$

In addition, $V(\boldsymbol{x})$ is continuous and continuously differentiable (except at singular surfaces) and $V(\boldsymbol{x})$ satisfies the Hamilton–Jacobi–Isaacs (HJI) equation.

Proof: We can obtain the partial derivatives of V with respect to each element of the state. They are given by

$$\begin{aligned} \frac{\partial V}{\partial x_E} &= \frac{m}{(1-\alpha^2)(m^2+1)} \cdot \frac{m(x_c - x_F) - (y_c - y_F)}{\sqrt{(x_c - x_F)^2 + (y_c - y_F)^2}} \\ &\quad - \frac{\alpha}{1-\alpha^2} \cdot \frac{x_E - x_P}{\sqrt{(x_E - x_P)^2 + (y_E - y_P)^2}} \\ \frac{\partial V}{\partial y_E} &= \frac{1}{(1-\alpha^2)(m^2+1)} \cdot \frac{-m(x_c - x_F) + (y_c - y_F)}{\sqrt{(x_c - x_F)^2 + (y_c - y_F)^2}} \\ &\quad - \frac{\alpha}{1-\alpha^2} \cdot \frac{y_E - y_P}{\sqrt{(x_E - x_P)^2 + (y_E - y_P)^2}} \\ \frac{\partial V}{\partial x_P} &= \frac{\alpha^2 m}{(1-\alpha^2)(m^2+1)} \cdot \frac{-m(x_c - x_F) + (y_c - y_F)}{\sqrt{(x_c - x_F)^2 + (y_c - y_F)^2}} \\ &\quad + \frac{\alpha}{1-\alpha^2} \cdot \frac{x_E - x_P}{\sqrt{(x_E - x_P)^2 + (y_E - y_P)^2}} \\ \frac{\partial V}{\partial y_P} &= \frac{\alpha^2}{(1-\alpha^2)(m^2+1)} \cdot \frac{m(x_c - x_F) - (y_c - y_F)}{\sqrt{(x_c - x_F)^2 + (y_c - y_F)^2}} \\ &\quad + \frac{\alpha}{1-\alpha^2} \cdot \frac{y_E - y_P}{\sqrt{(x_E - x_P)^2 + (y_E - y_P)^2}} \end{aligned} \tag{12}$$

Let us define the following:

$$\begin{aligned} \cos\eta &= \frac{x_F - x_c}{\sqrt{(x_F - x_c)^2 + (y_F - y_c)^2}}, \\ \sin\eta &= \frac{y_F - y_c}{\sqrt{(x_F - x_c)^2 + (y_F - y_c)^2}} \end{aligned} \tag{13}$$

so that $\tan\eta = \bar{m}$ as it can be seen in Fig. 3. Also define

$$\begin{aligned} \cos\lambda &= \frac{x_E - x_P}{\sqrt{(x_E - x_P)^2 + (y_E - y_P)^2}}, \\ \sin\lambda &= \frac{y_E - y_P}{\sqrt{(x_E - x_P)^2 + (y_E - y_P)^2}} \end{aligned} \tag{14}$$

where λ is the line-of-sight (LOS) angle from P to E.

Then, Eq. (12) can be written as follows:

$$\begin{aligned} \frac{\partial V}{\partial x_E} &= \frac{1}{1-\alpha^2}\left[\frac{m}{m^2+1}(-m\cos\eta + \sin\eta) - \alpha\cos\lambda\right] \\ \frac{\partial V}{\partial y_E} &= \frac{1}{1-\alpha^2}\left[\frac{1}{m^2+1}(m\cos\eta - \sin\eta) - \alpha\sin\lambda\right] \\ \frac{\partial V}{\partial x_P} &= \frac{\alpha}{1-\alpha^2}\left[\frac{\alpha m}{m^2+1}(m\cos\eta - \sin\eta) + \cos\lambda\right] \\ \frac{\partial V}{\partial y_P} &= \frac{\alpha}{1-\alpha^2}\left[\frac{\alpha}{m^2+1}(-m\cos\eta + \sin\eta) + \sin\lambda\right] \end{aligned} \tag{15}$$

Note that $\bar{m} = \tan\eta = (\sin\eta/\cos\eta)$. We then have that $m = -(1/\bar{m}) = -(\cos\eta/\sin\eta)$ and $m^2 + 1 = (1/\sin^2\eta)$. Additionally, $m\cos\eta - \sin\eta = -(1/\sin\eta)$ and Eq. (15) can be written in the simplified form:

$$\begin{aligned}
\frac{\partial V}{\partial x_E} &= -\frac{1}{1-\alpha^2}(\cos\eta + \alpha\cos\lambda)\\
\frac{\partial V}{\partial y_E} &= -\frac{1}{1-\alpha^2}(\sin\eta + \alpha\sin\lambda)\\
\frac{\partial V}{\partial x_P} &= \frac{\alpha}{1-\alpha^2}(\alpha\cos\eta + \cos\lambda)\\
\frac{\partial V}{\partial y_P} &= \frac{\alpha}{1-\alpha^2}(\alpha\sin\eta + \sin\lambda)
\end{aligned} \tag{16}$$

Note that the coordinates of the interception point I can be written as follows: $x_I = x_c + r\cos\eta$ and $y_I = y_c + r\sin\eta$. We can write

$$\begin{aligned}
\frac{x_I - x_E}{r} &= \alpha\cos\lambda + \cos\eta\\
\frac{y_I - y_E}{r} &= \alpha\sin\lambda + \sin\eta\\
\frac{x_I - x_P}{r} &= \frac{1}{\alpha}\cos\lambda + \cos\eta\\
\frac{y_I - y_P}{r} &= \frac{1}{\alpha}\sin\lambda + \sin\eta
\end{aligned} \tag{17}$$

By multiplying and dividing each equation in Eq. (11) by $1/r$, we obtain

$$\begin{aligned}
\cos\phi^* &= \frac{\alpha\cos\lambda + \cos\eta}{\sqrt{(\alpha\cos\lambda + \cos\eta)^2 + (\alpha\sin\lambda + \sin\eta)^2}}\\
\sin\phi^* &= \frac{\alpha\sin\lambda + \sin\eta}{\sqrt{(\alpha\cos\lambda + \cos\eta)^2 + (\alpha\sin\lambda + \sin\eta)^2}}\\
\cos\psi^* &= \frac{(1/\alpha)\cos\lambda + \cos\eta}{\sqrt{((1/\alpha)\cos\lambda + \cos\eta)^2 + ((1/\alpha)\sin\lambda + \sin\eta)^2}}\\
\sin\psi^* &= \frac{(1/\alpha)\sin\lambda + \sin\eta}{\sqrt{((1/\alpha)\cos\lambda + \cos\eta)^2 + ((1/\alpha)\sin\lambda + \sin\eta)^2}}
\end{aligned} \tag{18}$$

In general, the HJI equation is given by

$$-\frac{\partial V}{\partial t} = \frac{\partial V}{\partial \boldsymbol{x}}\cdot \boldsymbol{f}(\boldsymbol{x}, \psi^*, \phi^*) + g(t, \boldsymbol{x}, \psi^*, \phi^*) \tag{19}$$

In this problem we have that $(\partial V/\partial t) = 0$ and $g(t, \boldsymbol{x}, \psi^*, \phi^*) = 0$. Then, we compute

$$\begin{aligned}
&\frac{\partial V}{\partial x_E}\alpha\cos\phi^* + \frac{\partial V}{\partial y_E}\alpha\sin\phi^* + \frac{\partial V}{\partial x_P}\cos\psi^* + \frac{\partial V}{\partial y_P}\sin\psi^*\\
&= -\frac{\alpha}{1-\alpha^2}\cdot\frac{(\cos\eta + \alpha\cos\lambda)^2 + (\sin\eta + \alpha\sin\lambda)^2}{\sqrt{1+\alpha^2+2\alpha(\cos\lambda\cos\eta + \sin\lambda\sin\eta)}} + \frac{\alpha^2}{1-\alpha^2}\cdot\frac{(1/\alpha^2)(\alpha\cos\eta + \cos\lambda)^2 + (1/\alpha^2)(\alpha\sin\eta + \sin\lambda)^2}{(1/\alpha)\sqrt{1+\alpha^2+2\alpha(\cos\lambda\cos\eta + \sin\lambda\sin\eta)}}\\
&= \frac{\alpha}{1-\alpha^2}\cdot\frac{-(1+\alpha^2+2\alpha(\cos\lambda\cos\eta + \sin\lambda\sin\eta)) + 1 + \alpha^2 + 2\alpha(\cos\lambda\cos\eta + \sin\lambda\sin\eta)}{\sqrt{1+\alpha^2+2\alpha(\cos\lambda\cos\eta + \sin\lambda\sin\eta)}} = 0
\end{aligned} \tag{20}$$

In summary, the Value function $V(\boldsymbol{x})$ was obtained, it is continuous and continuously differentiable (outside dispersal surfaces), and it satisfies the HJI equation. □

Recall that the optimal strategies, as obtained in Proposition 1, were obtained from candidate strategies corresponding to each segment of the border. Each candidate solution is obtained by finding the closest point on the segment to the Apollonius circle whose radius and center are given by Eqs. (4) and (7), respectively. The closest point to the circle is obtained by means of the orthogonality condition in Proposition 1.

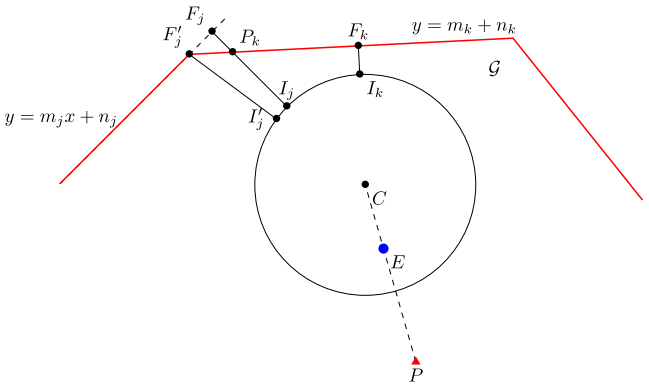

Fig. 4 Convex border.

When considering the candidate solution in the Euclidean plane and when the border is convex, there exist two cases: the closest point on segment j is such that $F_j \in \partial\mathcal{G}$ and the case where the point on the extended segment is such that $F_j \notin \mathcal{G}$. The second case is illustrated in Fig. 4 by drawing the extended line corresponding to segment j.

Corollary 1: If the closest point on segment j is such that $F_j \notin \mathcal{G}$, there exists $F_k \in \mathcal{G}$ such that $V_k(\boldsymbol{x}) < V_j(\boldsymbol{x})$. Hence, the point F_j is not the solution of the game and need not be considered in order to obtain the optimal strategies.

Proof: Consider $\boldsymbol{x} \in \mathcal{R}_p$ and consider the candidate solution $F_j \notin \mathcal{G}$. As it is shown in Fig. 4, it holds that $V_j(\boldsymbol{x}) = \overline{F_jI_j} > \overline{P_kI_j} > \overline{F_kI_k} = V_k(\boldsymbol{x})$, where P_k is the intersection point between segment k of the border and the line segment $\overline{F_jI_j}$. By the previous relationship, one can also discard any other point on segment j. For instance, since $F_j \notin \mathcal{G}$ is an infeasible solution, the point $F'_j \in \partial\mathcal{G}$ (in segment j) is the closest feasible point to the circle (to the corresponding point I'_j on the circle) and one may be tempted to consider this choice. However, we have that $\overline{F'_jI'_j} > \overline{F_jI_j}$ by definition of F_j; then, $\overline{F'_jI'_j} > \overline{F_kI_k} = V_k(\boldsymbol{x})$. □

B. Nonconvex Border

In this section we consider the existence of a nonconvex border. When the border is nonconvex, the case where the closest point on the extended segment j is such that $F_j \in \mathcal{G}$ is possible. This is now illustrated in Fig. 5. Point $F_j \in \mathcal{G}$ is an infeasible solution, because it does not lead the evader directly into safe haven. However, one can still consider the closest feasible point on segment j, which is point $N \in \partial\mathcal{G}$ in Fig. 5, the "corner" of the nonconvex border in consideration. Under this scenario we define

$$\begin{aligned}
V_j(\boldsymbol{x}) = &\sqrt{\left(\frac{1}{1-\alpha^2}(x_E - \alpha^2 x_P) - x_N\right)^2 + \left(\frac{1}{1-\alpha^2}(y_E - \alpha^2 y_P) - y_N\right)^2}\\
&-\frac{\alpha}{1-\alpha^2}\sqrt{(x_E - x_P)^2 + (y_E - y_P)^2}
\end{aligned} \tag{21}$$

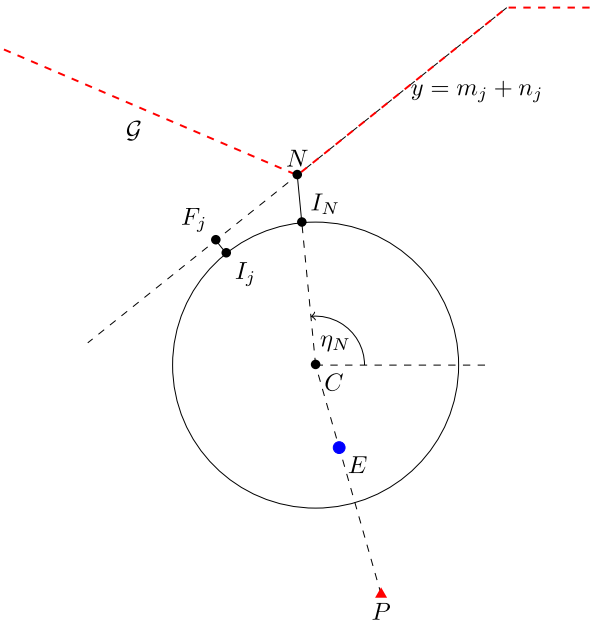

Fig. 5 Nonconvex border.

where the coordinates of point N are (x_N, y_N).

Corollary 2: Consider $\boldsymbol{x} \in \mathcal{R}_p$ and a nonconvex border where for segment j we have $V_j(\boldsymbol{x})$ as defined in Eq. (21). In addition, we consider the case where $i^* = j$; that is, the closest point on the border to the Apollonius circle is point N. Then, the Value function (21) is continuous and continuously differentiable (except at singular surfaces), and it satisfies the HJI equation.

Proof: The partial derivatives of the Value function with respect to each element of the state are given by

$$\begin{aligned}
\frac{\partial V}{\partial x_E} &= \frac{1}{1-\alpha^2}\cdot\frac{x_c - x_N}{\sqrt{(x_c-x_N)^2+(y_c-y_N)^2}} \\
&\quad - \frac{\alpha}{1-\alpha^2}\cdot\frac{x_E - x_P}{\sqrt{(x_E-x_P)^2+(y_E-y_P)^2}} \\
\frac{\partial V}{\partial y_E} &= \frac{1}{1-\alpha^2}\cdot\frac{y_c - y_N}{\sqrt{(x_c-x_N)^2+(y_c-y_N)^2}} \\
&\quad - \frac{\alpha}{1-\alpha^2}\cdot\frac{y_E - y_P}{\sqrt{(x_E-x_P)^2+(y_E-y_P)^2}} \\
\frac{\partial V}{\partial x_P} &= -\frac{\alpha^2}{1-\alpha^2}\cdot\frac{x_c - x_N}{\sqrt{(x_c-x_N)^2+(y_c-y_N)^2}} \\
&\quad + \frac{\alpha}{1-\alpha^2}\cdot\frac{x_E - x_P}{\sqrt{(x_E-x_P)^2+(y_E-y_P)^2}} \\
\frac{\partial V}{\partial y_P} &= -\frac{\alpha^2}{1-\alpha^2}\cdot\frac{y_c - y_N}{\sqrt{(x_c-x_N)^2+(y_c-y_N)^2}} \\
&\quad + \frac{\alpha}{1-\alpha^2}\cdot\frac{y_E - y_P}{\sqrt{(x_E-x_P)^2+(y_E-y_P)^2}}
\end{aligned} \tag{22}$$

Let us define in this case

$$\begin{aligned}
\cos\eta_N &= \frac{x_N - x_c}{\sqrt{(x_N-x_c)^2+(y_N-y_c)^2}}, \\
\sin\eta_N &= \frac{y_N - y_c}{\sqrt{(x_N-x_c)^2+(y_N-y_c)^2}}
\end{aligned} \tag{23}$$

and we can write Eq. (22) as follows:

$$\begin{aligned}
\frac{\partial V}{\partial x_E} &= -\frac{1}{1-\alpha^2}(\cos\eta_N + \alpha\cos\lambda) \\
\frac{\partial V}{\partial y_E} &= -\frac{1}{1-\alpha^2}(\sin\eta_N + \alpha\sin\lambda) \\
\frac{\partial V}{\partial x_P} &= \frac{\alpha}{1-\alpha^2}(\alpha\cos\eta_N + \cos\lambda) \\
\frac{\partial V}{\partial y_P} &= \frac{\alpha}{1-\alpha^2}(\alpha\sin\eta_N + \sin\lambda)
\end{aligned} \tag{24}$$

The coordinates of point I_N in Fig. 5 can be written as follows: $x_{I_N} = x_c + r\cos\eta_N$ and $y_{I_N} = y_c + r\sin\eta_N$. In addition, we can also obtain similar expressions to Eqs. (17) and (18) but in terms of η_N. Finally, the HJI equation is satisfied in a similar form to Eq. (20). □

C. Multiple-Pursuer Solution

The results from the previous section are now extended to the case of multiple pursuers. This is done primarily by making use of the solution to the minimum capture time problem for the two-pursuer [1,2] and multiple-pursuer [3] scenarios. In the minimum capture time two-pursuer, one-evader problem, depending on the initial conditions, the solution is for all three agents to head to the further of the two Apollonius circle intersections. For that game, it is also possible for the solution to degenerate to capture by a single pursuer; in this case, the presence of the second pursuer does not affect the outcome of the game. For more than two pursuers, Ref. [3] characterized the feasible region for the evader, that is, the set of points reachable by the evader before any of the pursuers. Let the Apollonius disk (i.e., the Apollonius circle and its interior) for the ith pursuer be given as

$$D_i = (r_i, (x_{C_i}, y_{C_i})) \tag{25}$$

where r_i is the radius of the Apollonius circle from Eq. (4) and (x_{C_i}, y_{C_i}) is the center of the Apollonius circle from Eq. (7). Then the evader's feasible region is defined as

$$S = \cap_{i=1}^{M} D_i, \qquad i = 1, \ldots, M \tag{26}$$

where M is the number of pursuers. Then let ∂S be the (inclusive) boundary of the region.

Proposition 2: Optimal capture must occur in S.

For any point outside of S, it cannot be guaranteed that the evader can reach the point before being captured (see [3,9]). Up to a point, increasing the number of pursuers has the effect of reducing the evader's feasible region, which is generally advantageous for the pursuers.

For the purposes of computing the multiple-pursuer solution, it is useful to reparameterize the border using an ordered set of points with a line segment joining consecutive points. Let B_i represent one such point, and then the border comprises line segments $B_{i,i+1}$ for $0 < i < K$, where K is the total number of corners of the border, including endpoints. Thus the border B is defined as a set of points along these line segments:

$$B \equiv \{(x,y) | \exists i \text{ s.t. } (x,y) \in B_{i,i+1}\} \tag{27}$$

We also restrict the border to be open, that is, $B_K \neq B_1$, and free of any self-intersections (i.e., no two segments cross).

In Sec. II.A it was shown that the closest point on a circle to line, say, $B_{j,j+1}$, can be found by drawing a line segment perpendicular to $B_{j,j+1}$ that terminates at the circle's center. The closest point I_j is then the intersection between this line segment and the circle. Similarly, F_j is the other endpoint of this line segment, incident to $B_{j,j+1}$. Repeating for all border segments $0 < j < K$ for a pursuer (say, pursuer i) yields a set of candidate capture points $\mathcal{I}_i = \{I_1, \ldots, I_{K-1}\}$ and their corresponding projection onto the border segment $\mathcal{F}_i = \{F_1, \ldots, F_{K-1}\}$. The optimal capture point for the single-pursuer problem is then given as

$$I^* = \arg\min_{I_j \in \mathcal{I}_i} \|I_j - F_j\| \tag{28}$$

For the multiple-pursuer case, the above procedure is repeated for each pursuer, but there are some additional caveats. As was shown in [1–3] optimal capture for the multiple-pursuer case may occur at the intersection of Apollonius circles. For the minimum capture time problem, it was also shown in [3] that capture may occur in the interior of S (i.e., in $S \cap \overline{\partial S}$) with three or more pursuers, but that is not the case here:

Lemma 1: Under optimal play, capture occurs on ∂S.

Proof: The distance from a point in any shape (e.g., S) to a point outside that shape (e.g., $(x, y) \in B$) is minimized at the boundary of that shape (e.g., ∂S). Because the evader's cost is the distance from the point of capture to the closest border segment, the evader would incur a loss by choosing a point on the interior of S. Points beyond ∂S cannot be optimal capture locations as stated in Proposition 2. □

One consequence of Lemma 1 is that the closest point on a pursuer's Apollonius circle does not correspond to a candidate capture point if that point is not in ∂S. Thus it is also required that for all I in $\mathcal{I}_i$ we have $I \in \partial S$. Second, because capture may occur at an intersection of Apollonius circles, we must also consider each of these points as candidate solutions by computing the smallest distance from each Apollonius circle intersection to each border segment. This is done similarly as before: draw a line segment that is perpendicular to the border segment whose endpoints are the border segment and the Apollonius circle intersection; the length of this line segment is the cost/payoff associated with this candidate solution. Let the set of Apollonius circle intersections be denoted as $\mathcal{I}_C$. Lastly, the orthogonality condition may yield a point F_j, which lies beyond one of the endpoints of the line segment. In these cases, F_j may be moved to the nearest endpoint (either B_j or B_{j+1}). The corresponding I_j (for an Apollonius circle) is the point on the circle that lies on the line connecting the circle center to F_j. This is especially pertinent in the case of a nonconvex border as these candidates may indeed be optimal. Algorithm 1 gives a sketch of the solution process.

Algorithm 1: MP1E border solution

procedure MP1E-BORDER $(\boldsymbol{x}, \alpha, B)$
  $S \leftarrow$ Compute evader's feasible region ▷see Eq. (26) and [3]
  $\mathcal{I}_C \leftarrow$ vertices of S ▷see [3]
  if $S \cap B$ **then**
    return ▷escape is possible
  end if
  $d \leftarrow \infty$
  $I^* \leftarrow (0, 0)$ ▷dummy initialization
  for all D_i Apollonius circles and I_k vertices $\in \mathcal{I}_C$ **do**
    for $j = 1, \ldots, K-1$ **do** ▷for each border segment
      Compute F ▷Eqs. (9) and (10) for Apollonius circles
      if F lies off of $B_{j,j+1}$ **then**
        $F \leftarrow \arg\ \min_{h \in j,j+1} \overline{FB_h}$
      end if
      if Apollonius circle, D_i **then**
        $I \leftarrow$ Compute the intersection of $\overline{FC}$ and ∂D_i
      else Vertex, $I_k \in \mathcal{I}_C$
        $I \leftarrow I_k$
      end if
      if $I \in \partial S$ **then**
        $d' \leftarrow \|I - F\|$
        if $d' < d$ **then** ▷update solution
          $d \leftarrow d'$
          $I^* \leftarrow I$
        else if $d' = d$ **then**
          $I^* \leftarrow [I^*, I]$ ▷nonunique solution
        end if
      end if
    end for
  end for
  return d, I^* ▷Value and capture point(s)
end procedure

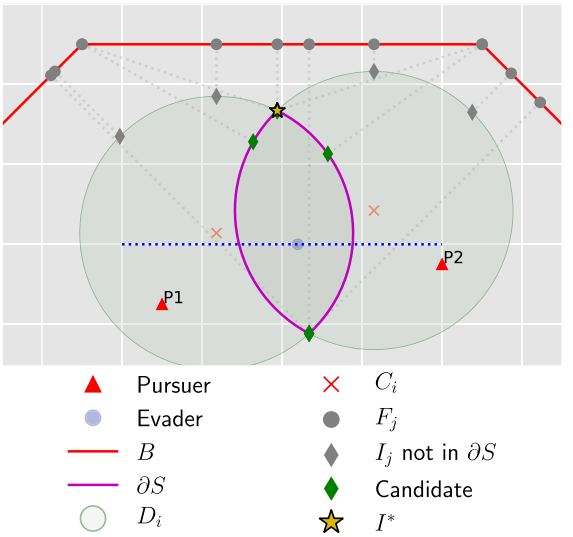

Fig. 6 The 2P1E scenario highlighting salient features in the solution process.

D. Examples

The first example, shown in Fig. 6, uses the same setup as in Fig. 1 with $\alpha = 0.6$. Essentially, the Value of the game is determined by comparing the lengths of all of the dotted gray lines emanating from the candidates. These are the lines of shortest length connecting the candidate to each border segment. It is clear by inspection of Fig. 6 that Algorithm 1 is inefficient: there are some lines that could not possibly be the shortest distance. Algorithm 1 contains a nested for-loop that has complexity $\mathcal{O}(MK)$, since the number of Apollonius circle intersections is at most M (i.e., $|\mathcal{I}_C| \leq M$). Using the parameterization of S given in [3], Algorithm 1 may be redesigned to achieve better worst-case performance (in a computational sense). We leave this exercise for future work.

The next example highlights the case where the border is nonconvex w.r.t the evader as well as degeneracy to capture by a single pursuer. Note that the optimal capture point I^* is closest to the corner of the border B_2. Incidentally, the line $F_1 I^*$ is not perpendicular to either border segment. In Fig. 7 pursuer P1 is not able to reach the optimal capture point at the same time as the evader and P2, and thus P1 and its Apollonius circle are shown in yellow. It just so happens that the Apollonius circle for P2 is contained entirely inside that of P1, and so ∂S is simply P2's Apollonius circle. Because of the shape of the border there is only one candidate solution. Here, P1 is free to do anything (including flee from the evader) without affecting the outcome of the game. These conditions are not necessary for degeneracy to capture by a single pursuer, however. Indeed it is possible for ∂S to be determined by several pursuers but still capture is undertaken by a single pursuer. In the latter case, the noncapturing pursuers may still need to aim for

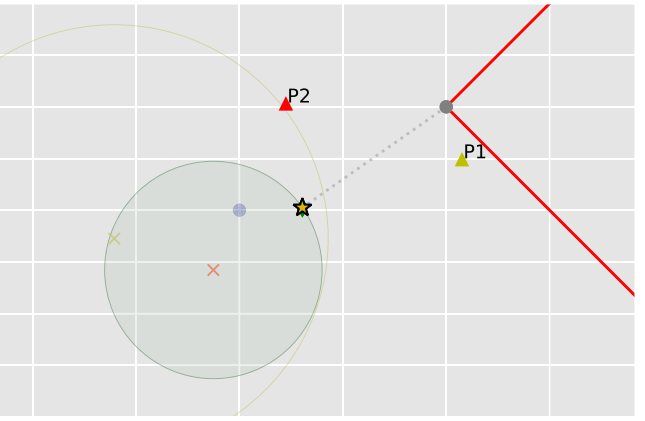

Fig. 7 The 2P1E scenario highlighting a nonconvex border as well as degeneracy to capture by a single pursuer. P1 and its Apollonius circle are shown in yellow to signify that P1 does not participate in capture.

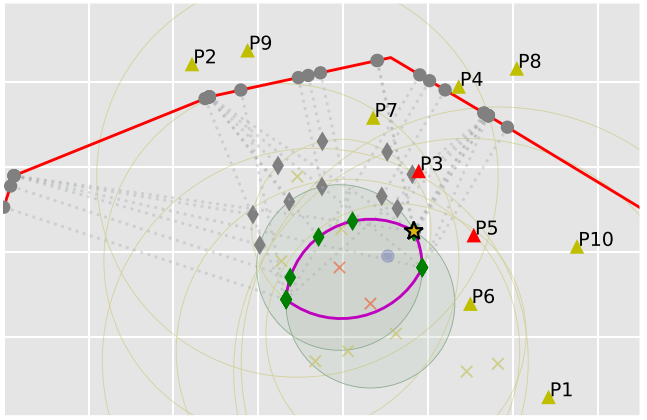

Fig. 8 The 10P1E example highlighting that capture is carried out by two pursuers.

the optimal capture point. The noncapturing pursuers cannot *reduce* the capture time; that is, they cannot improve the pursuers' objective. However, if the noncapturing pursuer(s) were to, for example, flee from the evader, it could be the case that a different point on ∂S becomes optimal. Such a switch may be beneficial (but never detrimental) to the evader. Reference [3] contains a more complete categorization of the pursuers in an MP1E scenario, which applies here as well. For the remainder, however, we only make a distinction between capturing (red) and noncapturing pursuers (yellow).

Figure 8 shows that even for large M (e.g., 10, in this case) capture is almost always carried out by two or one pursuers.

Remark: It is clear that only those pursuers whose Apollonius circles are a part of ∂S are pertinent to the solution of the game. Thus pursuers for which the following holds are discarded before invoking Algorithm 1:

$$\partial D_i \cap \partial S = \varnothing \tag{29}$$

The last example in this section, shown in Fig. 9, demonstrates the robustness of the policy from the perspective of the pursuer team. For this example, we choose to implement the agents' controllers in a discretized manner in order to visualize the response of the players to this type of implementation constraint. At each discrete time step, the pursuer recomputes the optimal capture point via Algorithm 1 and chooses its heading accordingly. In Fig. 9a the evader chooses to head straight to the border segment on the right, a choice that has some merit as it initially aims directly away from the pursuer and directly toward a border segment. Initially, the pursuer, unaware of the evader's implemented heading, heads toward the optimal capture point that is associated with the border segment on the left. At the fifth time step, there is a discrete switch to heading to a capture point associated with the border segment on the right. Although the suboptimal evader strategy allowed the evader to reach a point beyond S, the evader was not allowed to enter the red-shaded region. In fact, the saddle-point property of the Value function [Eq. (5)] guarantees this robustness. The same is true for the scenario in Fig. 9b, where the evader balances fleeing directly from the pursuer to avoid capture and heading directly toward the nearest border. Without solving the differential game, this latter strategy may seem like a good heuristic approach; however, the evader's cost is greater than the Value of the game.

III. Game of Kind

This section addresses the game of kind within the border defense differential game.

A. Single Pursuer

The solution of the game of kind characterizes the barrier surface $H(\boldsymbol{x}; \alpha, m_i, n_i)$ that separates the state space into the two regions: $\mathcal{R}_P$, the region of win of the pursuer, and $\mathcal{R}_E$, the region of win of the evader. If $\boldsymbol{x} \in \mathcal{R}_P$ the pursuer, playing optimally, is guaranteed to capture the evader before the latter reaches the border. On the other hand, if $\boldsymbol{x} \in \mathcal{R}_E$ the evader, playing optimally, is guaranteed to escape and reach the border before being captured by the pursuer.

We provide a visual representation on the Cartesian plane of the function $H(\boldsymbol{x}; \alpha, m_i, n_i)$, which specifies the surface that separates $\mathcal{R}_P$ from $\mathcal{R}_E$. By fixing the pursuer coordinates (x_P, y_P) we construct the closed form of the barrier surface $H(x, y; x_P, y_P, \alpha, m_i, n_i) = 0$. In other words, we characterize the coordinate pairs (x, y) of the possible evader position with respect to the pursuer coordinates that guarantee that E will escape P if E plays optimally. Let $\mathcal{R}_P, \mathcal{R}_E \subset \mathbb{R}^2$ denote the region of win of the pursuer and of the evader, respectively, in the Cartesian plane when P coordinates are fixed.

Theorem 2: Given the parameters (m_i, n_i) of segment i, for a given speed ratio parameter $0 < \alpha < 1$ and pursuer coordinates (x_P, y_P), the barrier surface cross section that divides the Cartesian plane into the two regions, R_P and R_E, with respect to segment i is given by the pursuer's side branch of the hyperbola

$$h_{xx}x^2 + h_{yy}y^2 + 2h_{xy}xy + 2h_x x + 2h_y y + h = 0 \tag{30}$$

where

$$\begin{aligned}
h_{xx} &= (1-\alpha^2)(m_i^2+1) - 1,\\
h_{yy} &= (1-\alpha^2)(m_i^2+1) - m_i^2,\\
h_{xy} &= -m_i,\\
h_x &= \alpha^2(x_P + m_i y_P) + (1-\alpha^2)m_i n_i,\\
h_y &= \alpha^2(x_P + m_i y_P)m_i - (1-\alpha^2)n_i,\\
h &= (1-\alpha^2)n_i^2 + \alpha^2(1-\alpha^2)[2n_i(y_P - m x_P)\\
&\quad - (m_i^2+1)(x_P^2 + y_P^2)] - \alpha^4(x_P + m_i y_P)^2
\end{aligned} \tag{31}$$

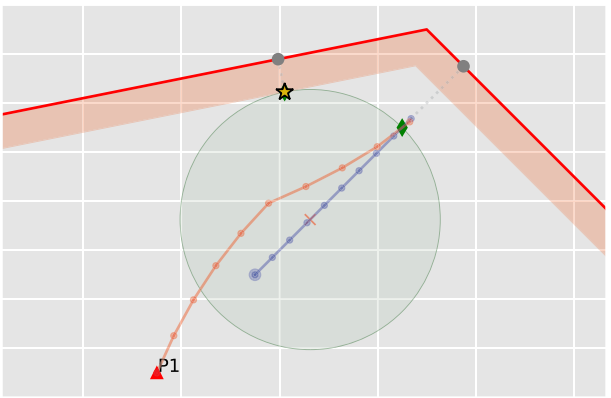

a) Evader chooses the suboptimal candidate; $V = 0.068$ and $J = 0.177$

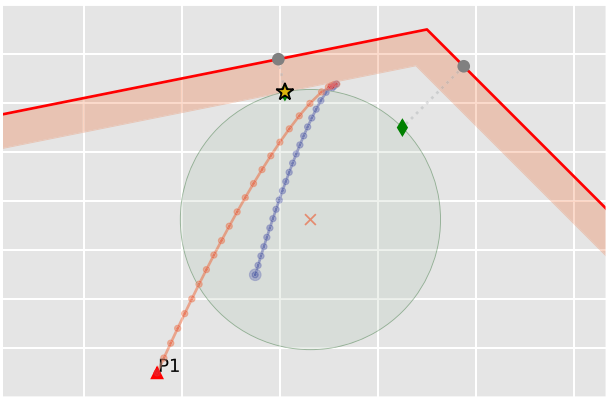

b) Evader mixes pure evasion with heading to nearest border; $V = 0.068$ and $J = 0.073$

Fig. 9 Optimal pursuit strategy against two different suboptimal evader strategies demonstrating robustness.

Proof: To determine the barrier surface with respect to segment i we consider the case where the Apollonius circle is tangent to segment i. The following condition holds

$$(x_c - x_F)^2 + (y_c - y_F)^2 = \frac{\alpha^2}{(1-\alpha^2)^2}[(x - x_P)^2 + (y - y_P)^2] \tag{32}$$

where the potential position of E is denoted by (x, y). Equation (32) can be written as follows:

$$\frac{1}{1-\alpha^2}(x^2 + y^2) - \frac{\alpha^2}{1-\alpha^2}(x_P^2 + y_P^2) + x_F^2 y_F^2 - 2(x_c x_F + y_c y_F) = 0 \tag{33}$$

Further, by writing (x_c, y_c, x_F, y_F) in terms of (x, y, x_P, y_P) and simplifying the resulting expression we obtain

$$\frac{1}{1-\alpha^2}(x^2 + y^2) - \frac{\alpha^2}{1-\alpha^2}(x_P^2 + y_P^2) + \frac{n_i^2}{m_i^2 + 1} - \frac{(x + m_i y - \alpha^2(x_P + m_i y_P))^2 + 2(1-\alpha^2)n_i(y - m_i x + \alpha^2(m_i x_P - y_P))}{(1-\alpha^2)^2(m_i^2 + 1)} = 0 \tag{34}$$

Multiplying the previous equation by $(1-\alpha^2)^2(m_i^2 + 1)$ and grouping the corresponding terms we obtain the quadratic equation (30). The discriminant of the quadratic equation (30) is given by

$$\begin{aligned} D &= \begin{vmatrix} (1-\alpha^2)(m_i^2+1) - 1 & -m \\ -m & (1-\alpha^2)(m_i^2+1) - m_i^2 \end{vmatrix} \\ &= (1-\alpha^2)^2(m_i^2+1)^2 - (1-\alpha^2)(m_i^2+1)^2 \\ &= -\alpha^2(1-\alpha^2)(m_i^2+1)^2 \\ &< 0 \end{aligned}$$

hence, Eq. (30) represents an hyperbola. □

Corollary 3: Given a point, N, of a nonconvex border, a given speed ratio parameter, $0 < \alpha < 1$, and pursuer coordinates, (x_P, y_P), the barrier surface cross section that divides the Cartesian plane into the two regions, R_P and R_E, with respect to point N is an arc of the circle

$$(x - x_N)^2 + (y - y_N)^2 = \alpha^2[(x_P - x_N)^2 + (y_P - y_N)^2] \tag{35}$$

Proof: The proof is similar to the proof for Theorem 2 and is omitted. □

To obtain the barrier surface for a collection of segments forming a convex border, one needs to compute the intersection of the corresponding hyperbolas/circles to each couple of adjacent segments.

B. Multiple Pursuers

Theorem 3 expresses a more general condition that determines the game of kind, which is applicable for both the single- and multiple-pursuer cases.

Theorem 3: Given the initial positions of the evader and pursuers, $\boldsymbol{x}$, and their respective speeds, if the border intersects the evader's feasible region, the evader is able to escape:

$$B \cap S \Rightarrow \boldsymbol{x} \in \mathcal{R}_E \tag{36}$$

where $\mathcal{R}_E$ is the region of win for the evader.

Proof: The Apollonius disk defines points that can be reached by the evader at or before a particular pursuer. Since S is defined as the set intersection of all of the Apollonius disks [c.f. Eq. (26)], the points in S are reachable by the evader at or before any pursuer, provided the evader takes an appropriate action. If the evader takes a straight-line path to the point, then every point along its path is also inside S due to the convexity of the region. Thus there always exists an *evasive path* (in the sense of [9]) for the evader to travel to a point in S. Therefore, since $B \cap S$ there exists $(x, y) \in B$ that is also in S, and so the evader can escape safely; that is, the pursuers cannot guarantee capture. □

Remark: If there is only one such point that meets the condition stated in Theorem 3, the border is tangent to S and capture occurs precisely at that point on the border.

Now we make use of these results to solve an example problem. Consider a border comprised of a single, infinitely long line with equally spaced UAVs flying along it in synchronized fashion, such that their spacing is always constant; the scenario is depicted in Fig. 10. The objective of the design problem is to defend the border by guaranteeing capture of any single intruder while minimizing cost. Cost, here, is monotonically increasing with the number of UAVs required (i.e., the density of UAVs along the border), the speed of the UAVs, and the sensing capabilities at the border. The cost may be considered as the monetary cost required to implement the border defense system. Thus our design variables are w, the half-distance between each UAV; α, the ratio of UAV speed to intruder speed; and d, the sensor range at the border. The spacing w is essentially half of the inverse of UAV density along the border; smaller w means more UAVs and higher cost. The variable d determines the distance inside the border that the laser fence is located; this distance essentially determines when the pursuit begins. In addition, for closed-loop optimal control in the sense of the differential game solution, all the positions of the agents must be known; thus the border's tracking sensors must have full coverage of the space between the laser fence and the border.

To solve the design problem, we make use of the solution of the game of kind for multiple pursuers. In particular, we find the critical point where capture occurs exactly at the border in the worst case. This critical point occurs when ∂S is tangent to the border, according to Theorem 3 and the subsequent remark. The best the evader can do is to start halfway in between the two pursuers; if evader starts any closer to either pursuer it will be captured further inside the border. This is because simultaneous capture occurs on the perpendicular bisector of $\overline{P1P2}$ (c.f. [10], in preparation). Thus, in order for the evader to minimize distance to the border at capture (i.e., maximize I_y), the evader must begin on the bisector. Any amount of horizontal distance traveled is akin to wasted time. For interception to occur exactly on the border, the following condition must hold:

$$C_{1_x}^2 + (d - C_{1_y})^2 = R_1^2 \tag{37}$$

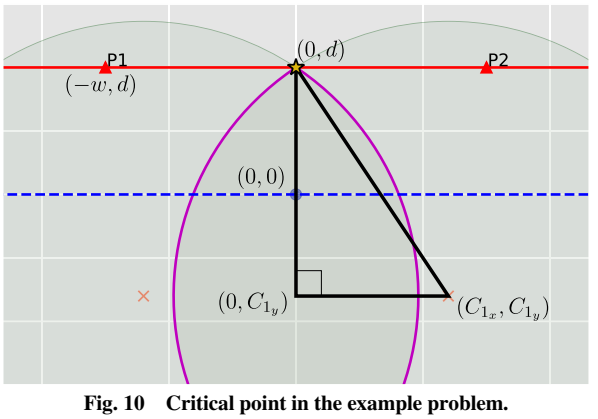

Fig. 10 Critical point in the example problem.

where

$$C_{1_x} = \frac{w\alpha^2}{1-\alpha^2}$$
$$C_{1_y} = \frac{-d\alpha^2}{1-\alpha^2}$$
$$R_1 = \frac{\alpha}{1-\alpha^2}\sqrt{w^2+d^2} \tag{38}$$

Note that Eq. (38) comes from the definition of the Apollonius circle. Substituting Eq. (38) into Eq. (37) and simplifying, we get

$$\alpha = \frac{d}{w} \tag{39}$$

Equation (39) also comes from the fact that the time of travel for pursuers and evader must be the same. At the critical point, the distance traveled by each pursuer is w and the distance traveled by evader is d, and so $w\alpha = d$. Therefore, given all but one of the parameters α, w, d we can determine the value of the free parameter from Eq. (39). If the design parameters do not satisfy Eq. (39) the system is either overdesigned (i.e., more costly than it ought to be) or cannot guarantee capture for all possible evader initial conditions.

IV. Dispersal Surface

A. Single Pursuer

For the single-pursuer case, when $V(\boldsymbol{x}) = \min_i V_i(\boldsymbol{x}) = V_k(\boldsymbol{x}) = V_l(\boldsymbol{x})$ for $k \neq l$, then a dispersal surface exists because more than one optimal solution exists. In general, there could be any number of optimal solutions where the region S is equidistant to multiple segments of the border and these distances are also the minimum. In such a case the Value function is continuous but it is not continuously differentiable since $(\partial V_k/\partial \boldsymbol{x}) \neq (\partial V_l/\partial \boldsymbol{x})$; for instance,

$$\begin{aligned}\frac{\partial V_k}{\partial x_E} &= \frac{m_k}{(1-\alpha^2)(m_k^2+1)} \cdot \frac{m_k(x_c - x_{F_k}) - (y_c - y_{F_k})}{\sqrt{(x_c - x_{F_k})^2 + (y_c - y_{F_k})^2}} \\ &\quad - \frac{\alpha}{1-\alpha^2} \cdot \frac{x_E - x_P}{\sqrt{(x_E - x_P)^2 + (y_E - y_P)^2}} \\ &\neq \frac{m_l}{(1-\alpha^2)(m_l^2+1)} \cdot \frac{m_l(x_c - x_{F_l}) - (y_c - y_{F_l})}{\sqrt{(x_c - x_{F_l})^2 + (y_c - y_{F_l})^2}} \\ &\quad - \frac{\alpha}{1-\alpha^2} \cdot \frac{x_E - x_P}{\sqrt{(x_E - x_P)^2 + (y_E - y_P)^2}} = \frac{\partial V_l}{\partial x_E}\end{aligned} \tag{40}$$

The main consequence is that the pursuers will see a small decrease of performance if they choose different from the evader. This is seen clearly in Fig. 11, where the evader is able to breach the red-shaded region if the pursuer aims at a different optima initially. Note that the cost/payoff, J, is equal to V if the agents aim at the same optima initially. In all other cases, $J < V$ representing a loss for the pursuer.

Table 1 Cost/payoff ($J \cdot 10^3$) for initial control action in Fig. 11

P\E	West	North	East
West	94	71	25
North	75	94	75
East	25	71	94

Interestingly, the loss in performance varies with the actual choices of the agents. Table 1 gives the cost/payoff for every combination of initial control action. West, north, and east denote aiming at the optima associated with these directions, respectively. Now we may treat the choice of initial heading and the values in Table 1 as a matrix game to determine the best choice of initial heading for the agents. The optimal strategies come from the Nash equilibrium (or equilibria), which may suggest that either a pure strategy or mixed strategy is optimal. It is obvious, in this case, that the pursuer's optimal strategy is to aim north, whereas the evader chooses either west or east with equal probability. Thus the optimal playout of the full game appears as in Fig. 11a or its mirror image. Although the Value of the differential game is 0.094, the presence of the dispersal surface results in a cost/payoff of 0.075, assuming optimal play of this matrix game followed by optimal play in the differential game. The values in Table 1 are dependent upon the time step. Smaller time steps will yield smaller losses relative to the Value of the game. However, for the scenario shown in Fig. 11, the Nash equilibrium and thus the optimal strategies of the initial matrix game are independent of the time step (unless, of course, the time step is so large that reaching the border can be achieved in a single step).

B. Multiple Pursuers

The possibility for a dispersal surface exists also for the multiple-pursuer case. As in the single-pursuer case, the dispersal surface is the result of multiple segments of the border. That is, this dispersal surface does not arise from the presence of multiple pursuers. If the border is made up of only one single segment, then the multiple-pursuer case does not contain a singular surface. Consider the scenario shown in Fig. 12, which has two pursuers and two optima. There is a horizontal border segment joining the two vertical segments far above, which does not affect the solution of the game. The pursuers, in addition to having to choose east or west, also must choose whether to agree on a direction or split up. Table 2 contains the values of the cost/payoff for two different time step sizes.

For the matrix game with $\Delta t = 0.10$, there is a single equilibrium wherein the pursuers' strategy is to both choose west or both choose east with equal probability, whereas the evader's strategy is to choose west or east with equal probability. This is not the case for $\Delta t = 0.15$. Using vertex enumeration (c.f. [11]) to compute the equilibria of the matrix game yields four different equilibria. Now there is the issue that a strategy is only optimal against the corresponding opponent strategy associated with a particular equilibrium. In some scenarios, there may exist a focal point (see [12]) wherein there is a particular equilibrium that is sensible for the players to agree upon. Interest-

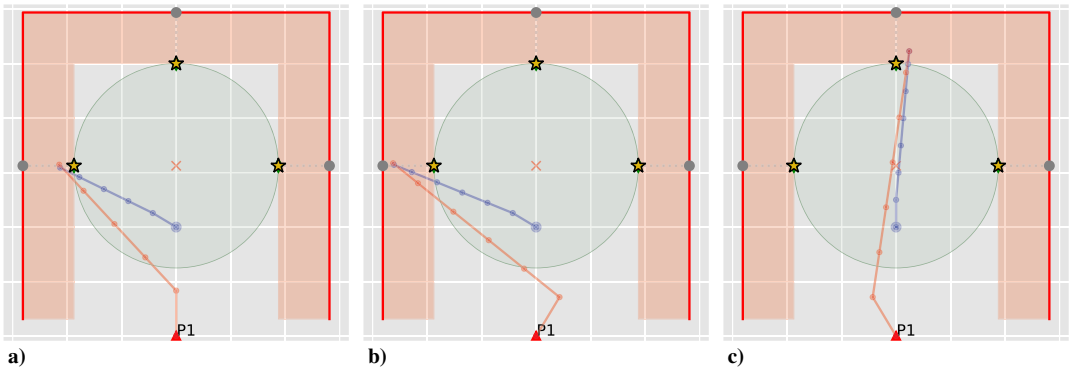

Fig. 11 Dispersal surface in a 1P1E scenario with three optimal capture points. Demonstration of agents choosing differently with $\Delta t = 0.05$ and $V = 0.094$.

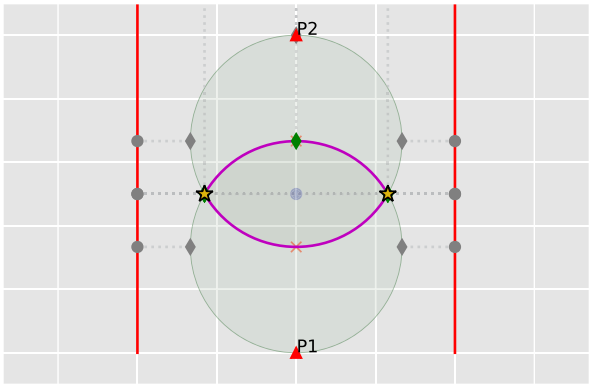

Fig. 12 Dispersal surface in a 2P1E scenario with two optimal capture points.

Table 2 Cost/payoff ($J \cdot 10^3$) for initial control action in Fig. 12

$\Delta t = 0.10$			$\Delta t = 0.15$		
P1/P2 \ E	W	E	P1/P2 \E	W	E
W/W	211	206	W/W	211	201
W/E	208	208	W/E	206	206
E/W	208	208	E/W	206	206
E/E	206	211	E/E	201	211

ingly, for the present case, all four equilibria have a pursuer strategy of splitting up. This is intuitive—the potential loss associated with both pursuers choosing opposite the evader is much greater for $\Delta t = 0.15$ than it is for $\Delta t = 0.10$; thus, splitting up is the best option here.

Finally, we note that the *perpetual dilemma*, as described by Isaacs [1], does not appear to occur in this game. That is to say, after the agents make a choice of initial heading, regardless of the choices made, the system state will move off of the dispersal surface.

V. Conclusions

In this paper, a multiple-pursuer, single-evader differential game has been formulated and solved with a practical application to border defense. This paper considered an intruder who is attempting to escape through the border with some valuable intelligence; the border is guarded by one or more UAVs, whose goal is to capture the evader (if possible) as far inside the border as possible. For the case of multiple UAVs, or pursuers, strategies that maximize the cooperation were sought. Treating the scenario as a two-player differential game played by the intruder and the team of UAVs lead to the desired result. In the game of degree, capture can be guaranteed, and the cost/payoff is the smallest distance from the point of capture to any segment of the border. Using the well-known Apollonius circle, the Value function for the single-pursuer, single-evader game was expressed analytically and shown to satisfy the HJI equation. In this way, the solution was verified. The single-pursuer solution was extended to multiple pursuers by considering simultaneous capture by two or more pursuers at the intersection of their Apollonius circles. These candidate solutions behave much the same way as the single-pursuer candidate solutions. A simple approach was expressed to determine the optimal capture point for given initial conditions, which, in turn, determines the Value of the game and the optimal headings for all the agents. For the game of kind, conditions that can be easily checked were expressed to determine in which region a given initial condition lies (whether in the evader or pursuers' win region). Finally, this paper characterized the dispersal surface in this game and presented optimal strategies for the evader and pursuers for choosing an initial heading.

The solution of the differential game posed in this paper could have many applications, one of which was illustrated in the example problem. There are also many possible extensions to this work, including multiple intruders, a heterogeneous pursuer team, intruder with escorts, and static border defenses, which are left for future research. The benefits of considering such scenarios in the context of differential games are that cooperation among a team of agents is maximized, the strategies for both players are robust to any opponent strategy, and analytical solutions (if they may be found) could be implemented onboard in real time.

Acknowledgment

This paper is based on work performed at the Air Force Research Laboratory (AFRL) *Control Science Center of Excellence*. Distribution Unlimited. 4 June 2018. Case #88ABW-2018-2891.

References

[1] Isaacs, R., *Differential Games: A Mathematical Theory with Applications to Optimization, Control and Warfare*, Wiley, New York, 1965, Chap. 1.

[2] Garcia, E., Fuchs, Z. E., Milutinović, D., Casbeer, D. W., and Pachter, M., "A Geometric Approach for the Cooperative Two-Pursuer One-Evader Differential Game," *IFAC-PapersOnLine*, Vol. 50, No. 1, 2017, pp. 15209–15214. https://doi.org/10.1016/j.ifacol.2017.08.2366

[3] Von Moll, A., Casbeer, D. W., Garcia, E., and Milutinović, D., "Pursuit-Evasion of an Evader by Multiple Pursuers," *2018 International Conference on Unmanned Aircraft Systems (ICUAS)*, IEEE, New York, 2018, pp. 133–142. https://doi.org/10.1109/ICUAS.2018.8453470

[4] Huang, H., Zhang, W., Ding, J., Stipanović, D. M., and Tomlin, C. J., "Guaranteed Decentralized Pursuit-Evasion in the Plane with Multiple Pursuers," *2011 50th IEEE Conference on Decision and Control and European Control Conference (CDC-ECC)*, IEEE, New York, 2011, pp. 4835–4840.

[5] Zhou, Z., Zhang, W., Ding, J., Huang, H., Stipanović, D. M., and Tomlin, C. J., "Cooperative Pursuit with Voronoi Partitions," *Automatica*, Vol. 72, Suppl. C, 2016, pp. 64–72. https://doi.org/10.1016/j.automatica.2016.05.007

[6] Oyler, D. W., Kabamba, P. T., and Girard, A. R., "Pursuit-Evasion Games in the Presence of Obstacles," *Automatica*, Vol. 65, Suppl. C, 2016, pp. 1–11. https://doi.org/10.1016/j.automatica.2015.11.018

[7] Oyler, D., "Contributions to Pursuit-Evasion Game Theory," Ph.D. Thesis, Univ. of Michigan, Ann Arbor, MI, 2016.

[8] Pashkov, A. G., and Terekhov, S. D., "A Differential Game of Approach with Two Pursuers and One Evader," *Journal of Optimization Theory and Applications*, Vol. 55, No. 2, 1987, pp. 303–311. https://doi.org/10.1007/BF00939087

[9] Cheung, W. A., "Constrained Pursuit-Evasion Problems in the Plane," Ph.D. Thesis, Univ. of British Columbia, Vancouver, BC, 2005.

[10] Pachter, M., Von Moll, A., Garcia, E., Casbeer, D., and Milutinović, D., "Two-on-One Pursuit," *Journal of Guidance, Control, and Dynamics*, Vol. 42, No. 7, July 2019. https://doi.org/10.2514/1.G004068

[11] Avis, D., Rosenberg, G. D., Savani, R., and von Stengel, B., "Enumeration of Nash Equilibria for Two-Player Games," *Economic Theory*, Vol. 42, No. 1, 2010, pp. 9–37. https://doi.org/10.1007/s00199-009-0449-x

[12] Schelling, T. C., *The Strategy of Conflict*, Harvard Univ. Press, Cambridge, MA, 1980, Chap. 3.

J. P. How
Associate Editor